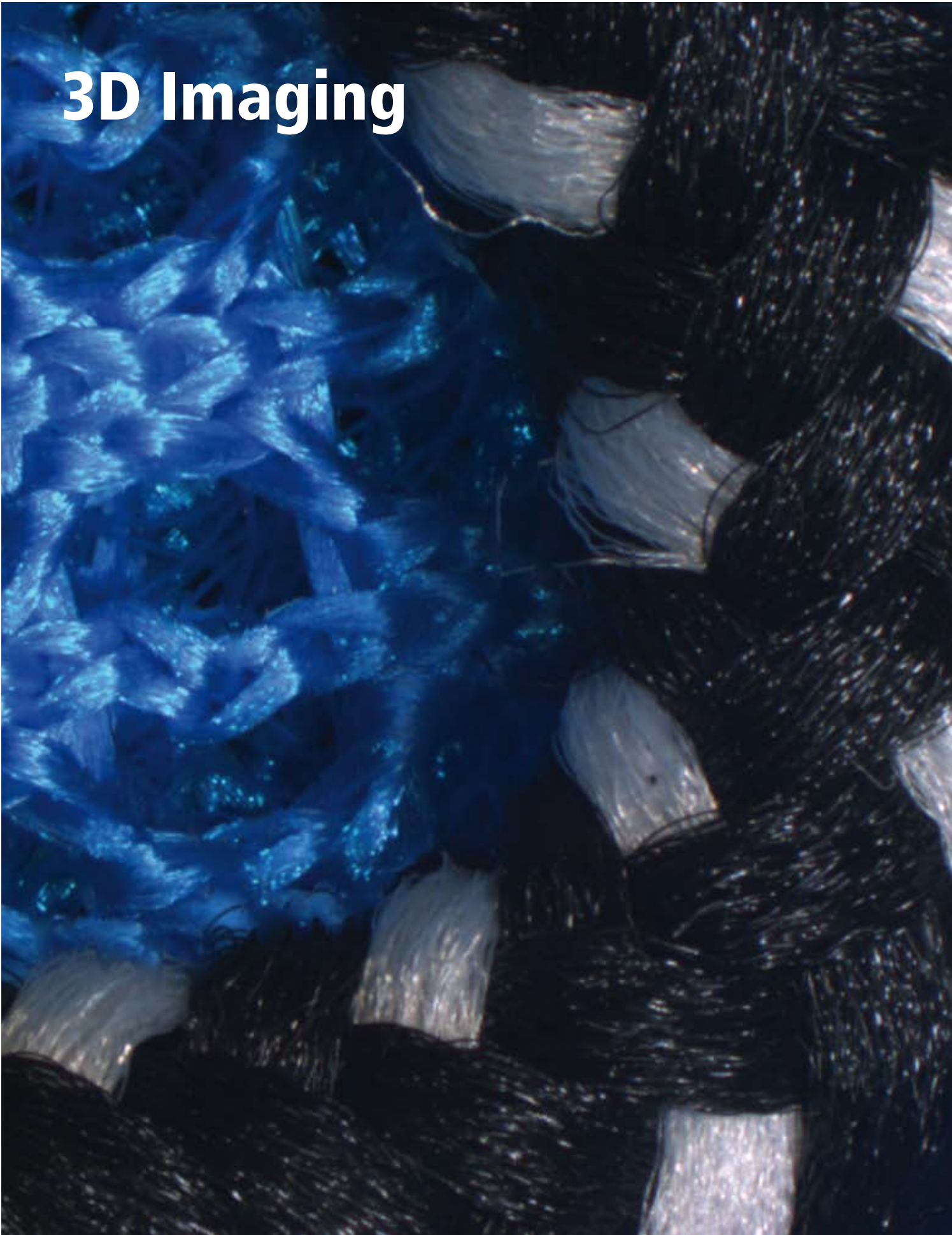


# 3D Imaging





## Reality is multi-dimensional

What do we see when we observe a sample through a light microscope? What information do we perceive? Most light microscopes give us a two-dimensional view of physical reality. What we usually observe in the widefield microscope is the projection of a three-dimensional physical structure down to a two-dimensional image. This means one dimension is lost which significantly restricts our perception of the physical reality viewed.

When looking at two dimensional images we often reverse the process and, based on experience, more or less unconsciously extend the two dimensional view into the third dimension. But how can we be sure that this interpretation is accurate? While watching the night sky we cannot tell whether two stars are close to each other or are in fact hundreds of light years away in space. Painting techniques, however, offer numerous examples of how to create a distinct impression of a third dimension using different lighting and shading of contrast, as well as well-placed usage of objects with familiar proportions. The fact that we are accustomed to recognising different lighting on a structure in a three dimensional way is also how relief is shown – such as in contrast methods used in microscopy (e.g. Differential Interference Contrast (DIC)).

## The stereo view

Our eyes always view objects from a slight angle defined by the distance of our eyes and the distance between the object and us. Together with the interpretation that our brain provides us with, this creates a three-dimensional view with these two sources of perception. To see objects within a microscope in a similar way, both eyes have to each be provided with a separate light path to enable observation of the specimen at an angle similar to the one our eyes see from naturally. This is exactly what stereo microscopy is all about. These microscope types, often called “binos”, provide a view of a specimen that looks natural, including a high depth of field and working distance. With a convergence angle of 10–12°, the left eye and right eye receive views of the same object from a slightly different perspective (fig. 54).

For viewing surfaces, the stereo microscope provides a reliable three-dimensional impression of the object. We get an idea of how the surface is shaped and which structures are higher or lower. What we are investigating here is a

curved, two-dimensional surface expanded into three dimensional space. However, one general restriction is still the limited depth of field which makes it often impossible to obtain a completely sharp image. Additionally, stereo microscopes are restricted in magnification and resolving power due to their general design when compared with upright or inverted widefield microscopes. Furthermore, when using a stereo microscope for documenting images, only one of the microscope pathways will be used for the camera in most cases. This means the resulting digital image is only two-dimensional – there is no third dimension.



**Fig. 54:** The stereomicroscopic (Galileo type) light path – two microscopes in one – offers observation of specimens at the natural convergence angle of our eyes. This makes the 3D topography visible. However, when the specimen is documented the image will nevertheless remain a two-dimensional view.

Thus, when we want to have a sharp view of a topographic structure in light or stereo microscopes – or in general, when we want to know more about the three-dimensional internal set-up of structures, several sections or slices have to be acquired. All at a different z position or on a different focal plane. Have a look at an image stack containing several such sections of the human head acquired via Magnetic Resonance Imaging (MRI) (fig. 55).

## Not too few – Not too many – just enough

Using the light microscope, optical sections are usually acquired using a motorised focus. First the maximum and the minimum position along the z axis of the stage or the nosepiece are defined. Then you either set the distance of two z-positions (i.e. the focal change ( $\Delta z$ ) or z spacing), or you set the total number of sections to acquire. Depending on the application, a minimum number of sec-

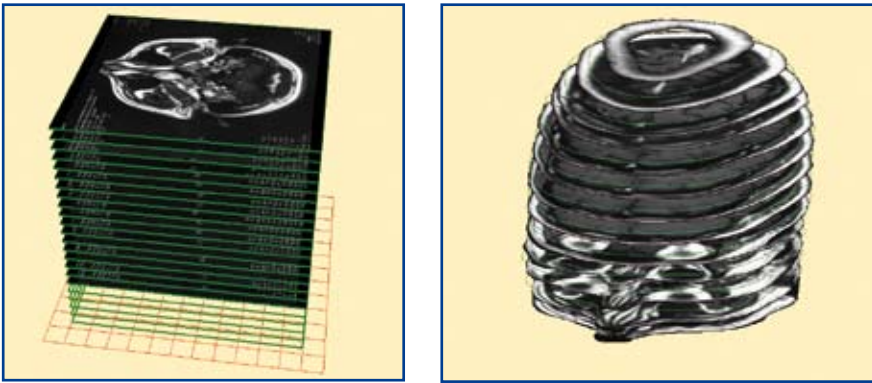


**Fig. 55:**  
**Left:** Stack of images taken via MRI (Magnetic Resonance Imaging).  
**Right:** The head structures are extracted from the individual image sections.

tions with the optimum  $\Delta z$  spacing ( $\Delta z$ ) will be necessary.

One application in light and stereo microscopy is the acquisition of  $z$  stacks for overcoming the limited depths of field of a single frame. This is where the focal change ( $\Delta z$ ) between two sections should be the same or somewhat smaller than the depth of field. As described above, the depth of field depends mainly on the numerical aperture of the objective. In practice, a usable  $\Delta z$  value can be easily derived by lifting the stage slowly. At the same time, you observe at which focal change a sharp structure goes out of focus. You apply this value to all the sections over the whole height range of your sample (fig. 56). With digital imaging, the focus parameters can be entered; the software takes control of the motorised focus and acquires the  $z$  stack. The focused areas through the sections can then be composed to generate an image which has an unlimited depth of field in principle (fig. 56). The method referred to is called EFI (Extended Focal Imaging). (See also box 6)

In addition to the resulting image (fig. 56) with an unlimited depth of field, a height map can be generated (fig. 57). The software algorithm knows which section to obtain the sharp pixels from to

compose the resulting image. This information is used to create an image where each grey value represents a specific height. This height map contains as many grey value levels as sections have been acquired. This means that the smaller the depth of field of your objective and the more sections actually acquired, the more exact the height information will be. This is significant when the height information is represented in a three-dimensional view (fig. 57). When a sufficient number of sections are acquired, the viewer receives a clear spatial impression of the surface. To smoothen the height map, peaks and steps may be flattened somewhat. The three-dimensional view becomes quite a realistic representation of the actual object structure when the sharp, composite image is placed over the surface as a texture (fig. 57).

### Just the right number

In life science applications and fluorescence microscopy, the appropriate number of sections for three-dimensional imaging can also be derived from the experimental set-up. It is well known that out-of-focus haze can significantly diminish fluorescence images' scientific value, as well as the apparent clarity in fluores-

cence images acquired in standard fluorescence widefield microscopes. There are two main techniques used to remove this out-of-focus blur and to restore the images: the deconvolution computational technique and confocal microscopy. One of these approaches is desirable to create a reasonable three-dimensional representation of the fluorescence signals.

Deconvolution requires a three-dimensional image stack of the observed sample, having a minimum focal change ( $\Delta z$ ) for obtaining maximum effect. The focal change ( $\Delta z$ ) depends on the numerical aperture (NA) of the objective, the sample fluorochrome's emission wavelength ( $\lambda$ ) and the refractive index ( $n$ ) of the immersion medium, and can be calculated using the following equation:

$$\Delta z \sim (1.4 * \lambda * n) / NA^2 \quad (7)$$

To get a better idea of the actual numbers, an example will be calculated. A Plan Fluorite 40x objective has an NA value of 0.75. The refractive index of air is 1. At 540 nm emission wavelength, this yields a minimum required focal change, i.e.  $z$  spacing ( $\Delta z$ ) of about 1.3  $\mu\text{m}$ . The numerical aperture mostly influences the  $z$  spacing. When using a higher quality Plan Achromat objective with a numerical aperture (NA) of 0.9, a  $z$  spacing ( $\Delta z$ ) of about 0.9  $\mu\text{m}$  is required. When observing cells, a height range of 5 to 10  $\mu\text{m}$  must be covered depending on cell type and preparation. So when using a Plan Achromat 40x objective, up to 10 sections or frames should be acquired. Fig. 58 shows an example.

Software solutions available today offer either definition of the numerical aperture and the refractive index. With fully motorised systems, the software also reads out the numerical aperture and the refractive index of the current objective. When the fluorochrome is selected, the  $z$  spacing is automatically calculated. You define the maximum and

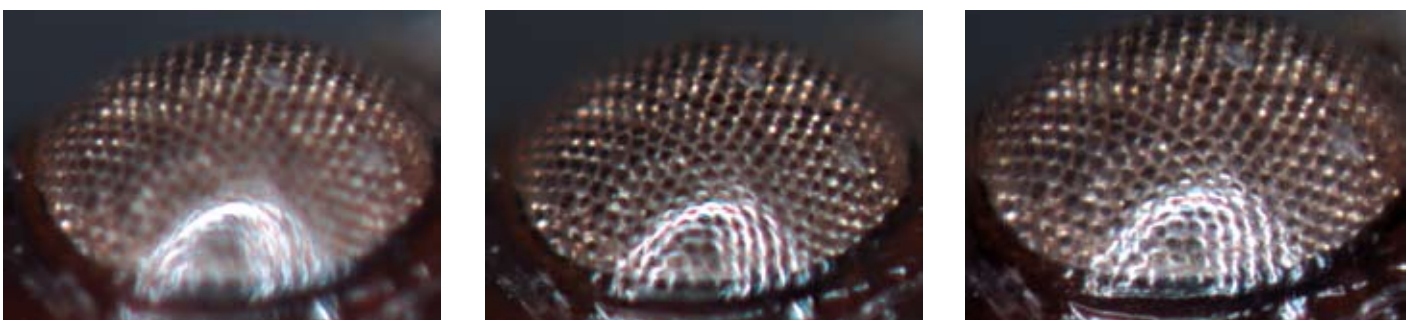


**Fig. 56:**  
**Left and middle:** This is an eye of a beetle acquired at two different focal planes. The focal change ( $\Delta z$ ) is such that no structure between these focal planes is not sharply in focus.  
**Right:** Seven optical sections acquired at different focal planes are combined to create one sharp image with unlimited depth of field.

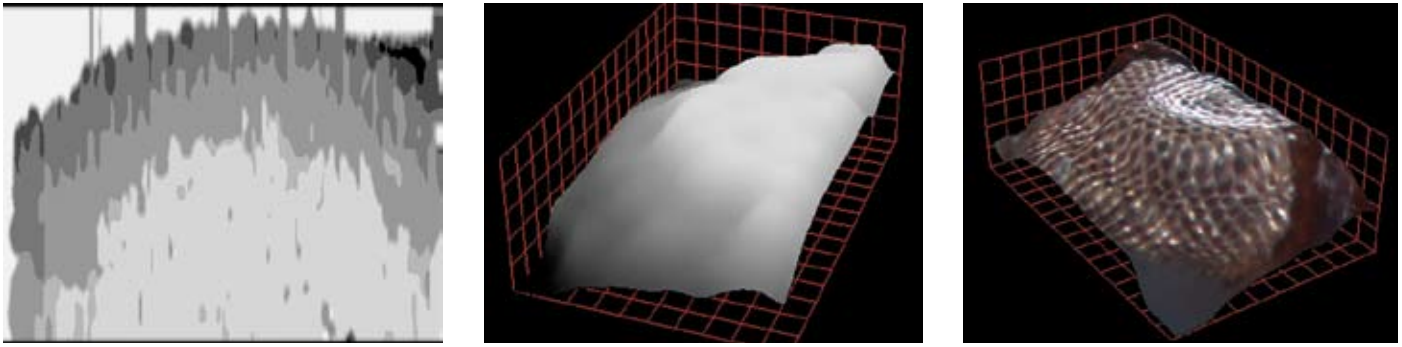


Fig. 57: Left: Height map. Middle and right: Three-dimensional view of the surface. The surface shape can be textured with the composite image.

the minimum lift of the stage and the z stack is acquired.

The deconvolution filter can be directly applied to the z stack image object. The most powerful deconvolution filter is called blind deconvolution. It does not assume any prior knowledge of the system or sample. Instead, it uses elaborate and time consuming mathematical iterative approaches. These include the constrained maximum likelihood estimation method to adapt to the actual three-dimensional point spread function (PSF) of the system (for a more detailed description see the paragraph „What exactly is a point spread function“ in the chapter „The Resolving Power“). Knowing the three-dimensional PSF of a system, the blind deconvolution takes the blurred z stack and essentially provides a three-dimensional image restoration of the sample (fig. 58, 60, 62). Deconvolution algorithms are applied to a lesser degree in confocal microscopy image stacks and to images from transmitted light widefield microscopy as well.

### The confocal view

The second way to create optical sections in a fast and high resolution manner is via confocal microscopy. Here, a light beam, usually a laser, is concentrated on a small area of the specimen. The light originating from this spot (emission light of the fluorescence or reflected light of opaque materials) is captured by a sensitive detector. Within the confocal optics, an aperture (usually a pin hole) is placed at a position which is optically conjugated with the focusing position. This conjugated focal position set-up is why the term “confocal” is used (see also Box 4). The system is meant to eliminate light from all areas other than that on the focal plane. Therefore, while scanning along x, y axes, an optical section of the focused area can be obtained without requiring software algorithms.

### One for all

Today’s software generally handles the z stack as one object. All sections and frames are saved in a single file. The information about the single frames’ x-y resolution and calibration, as well as the z spacing and the other meta-data such as the channel (fluorochrome and wavelength), point in time acquired, numerical aperture and refractive index are saved in the same file as well. The single layers can be viewed separately or extracted. A quick way to display all the significant structures through the whole stack is the maximum intensity projection. This is where the brightest pixel value at each x-y position throughout all layers is shown in the projection image (fig. 58, 60, 62). Other projection methods are mean intensity and minimum intensity projections.

Projection methods have to be used with care because the lack of out-of-focus blur shows all details from the various z-levels as if they were all located on the same horizontal plane – which is obviously not the case. For readers viewing such images in a scientific journal, a

seemingly satisfactory multicolour confocal two-dimensional image will in fact reveal less valid information than a “normal” widefield fluorescent image. Another way of presenting stacks is by animating them – like watching a movie. Image objects are truly multi-dimensional. In addition to the third axis in space, they may also contain different colour channels of multiply labelled fluorescent specimens – the fourth dimension (fig. 59, 60 and 62). Image objects may also be comprised of a fifth dimension – time: where slices are acquired at different points in time.

### It’s all spatial

Z stacks and multidimensional images can be visualised as three-dimensional objects via three-dimensional volume rendering, or voxel viewing. Voxel stands for Volume Element. Fig. 61 shows the correspondence between pixel and voxel. A voxel is a pixel which has a height value additionally assigned to it. The height assigned corresponds to the z spacing of the frames. In this way, voxels are reconstructed from the frames of the z stack.

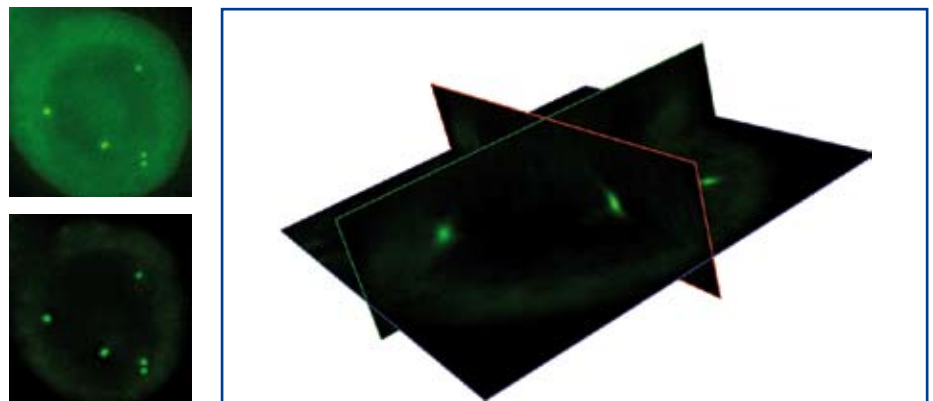


Fig. 58: Human breast cancer tissue labelled with a probe against the HER2-gene (Texas Red – not shown here, see fig. 62) and Chromosome 17 (FITC).  
 Upper left: Maximum intensity projection of 25 frames,  $\lambda(\text{FITC}) = 518 \text{ nm}$ , numerical aperture  $\text{NA} = 1$ , z spacing ( $\Delta z$ ) = 0.18.  
 Lower Left: The same z stack after applying the blind deconvolution algorithm. Right: The three-dimensional slice view gives a good impression of the proportions and helps to spatially locate the fluorescence signals.

Each voxel of a three-dimensional object has a colour. There are several well-known methods for volume rendering, such as projection and ray casting. These approaches project the three-dimensional object onto the two-dimensional viewing plane. The correct volume generating method guarantees that more than just the outer surface is shown and that the three-dimensional object is not displayed simply as a massive, contourless block. Inner structures within a three-dimensional object, such as fluorescence signals can be visualised. The maximum intensity projection method looks for the brightest voxel along the projection line and displays only this voxel in the two-dimensional view. Fig. 62 shows the maximum intensity projection of two colour channels of 25 frames each when seen from two different angles. Changing the perspective helps to clearly locate the fluorescence signals spatially. The three-dimensional structure will appear more realistic when the structure rendered into three-dimensions is rotated smoothly.

### How many are there – One or Two?

Managing several colour channels (each having many z layers) within one image object can be deceptive. The question is whether two structures appearing to overlap are actually located at the same position spatially or whether one is in fact behind the other. The thing is, two fluorescence signals may overlap – because their mutual positions are close to each other within the specimen. This phenomenon is called colocalisation. It is encountered when multi-labelled molecules bind to targets that are found in very close or spatially identical locations.

Volume rendering makes it possible to locate colocalised structures in space visually. For better representation and in order to measure colocalisation in digital image objects, the different fluorescence signals are first distinguished from the background. This may be done via

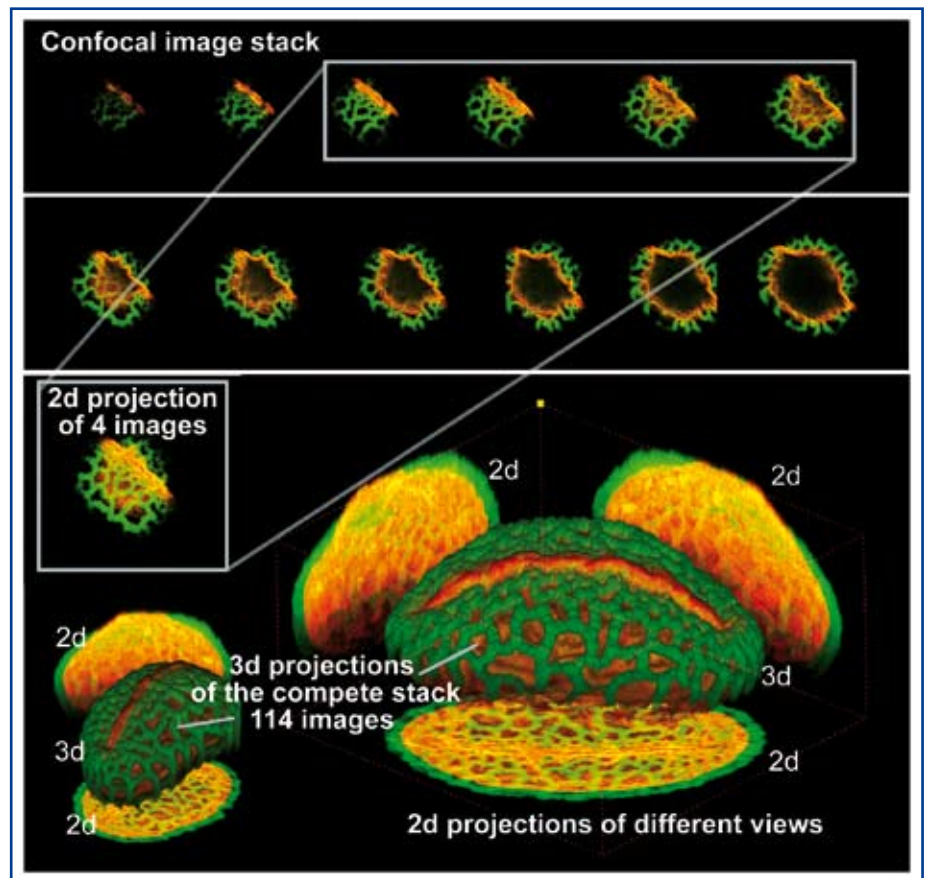


Fig. 59: Confocal images of pollen. The upper rows show the first 12 images of a series of 114, that can be used to create either two-dimensional projections of parts of the pollen or create a 3D view of the surface structure. This three-dimensional projection shown here is accompanied by two-dimensional projections as if the pollen was being viewed from different perspectives. Images were created using the Olympus Fluoview 1000.

threshold setting in each of the colour channels. A new image object can be created with only those structures that were highlighted by the thresholds. The colocalised fluorescence signals are displayed in a different colour. Rendering these image objects clearly reveals the colocalised signals without any background disturbance. To obtain quantitative results, the area fraction of the colocalised signals compared to the total area of each of the two fluorescence signals can be calculated throughout all image sections (see table 4).

### 3-D reconstructions

Now let us draw the net wider and move for a minute beyond the light microscopy approaches in imaging three-dimensional objects. In general, determining three-dimensional structures from macro to atomic level is a key focus for current biochemical research. Basic biological processes, such as DNA metabolism, photosynthesis or protein synthesis require the coordinated actions of a large number of components. Understanding the three-dimensional organisation of these components, as well as their detailed atomic structures, is crucial to being able to interpret what their function is.

In the materials science field, devices have to actually „see“ to be able to measure three-dimensional features within materials, no matter how this is done: whether structurally, mechanically, electrically or via performance. However, as the relevant structural units have now moved to dimensions less than a few hundred nanometres, obtaining this three-dimensional data means new methods have had to be developed in order to be able to display and analyse

Table 4:

Layer	Red Area[%]	Green Area[%]	Colocalisation Area[%]	Colocalisation/Red Ratio[%]	Colocalisation/Green Ratio[%]
1.00	0.11	0.20	0.04	39.60	21.22
2.00	0.15	0.26	0.07	47.76	27.92
3.00	0.20	0.36	0.10	49.93	28.08
4.00	0.26	0.53	0.13	51.84	25.32
5.00	0.35	1.34	0.20	57.39	14.87
6.00	0.43	2.07	0.26	61.00	12.81
7.00	0.38	1.96	0.24	61.66	12.07

Colocalisation sheet: A ratio value of about 52 % in the Colocalisation/Red column in layer 4 means that 52 % of red fluorescence signals are colocalised with green fluorescent structures here.

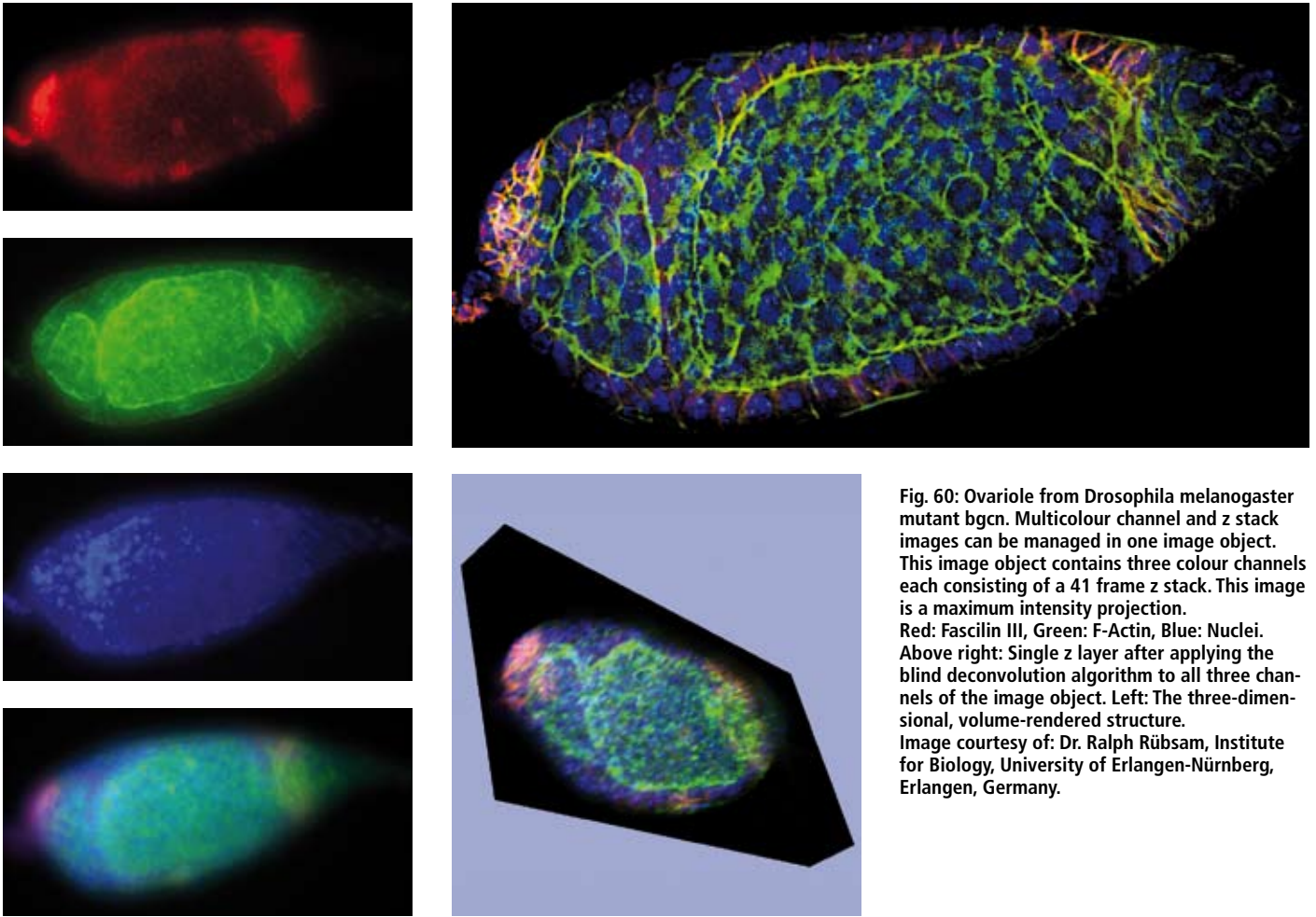


**Fig. 60:** Ovariole from *Drosophila melanogaster* mutant *bgcn*. Multicolour channel and z stack images can be managed in one image object. This image object contains three colour channels each consisting of a 41 frame z stack. This image is a maximum intensity projection. Red: Fascilin III, Green: F-Actin, Blue: Nuclei. Above right: Single z layer after applying the blind deconvolution algorithm to all three channels of the image object. Left: The three-dimensional, volume-rendered structure. Image courtesy of: Dr. Ralph RübSam, Institute for Biology, University of Erlangen-Nürnberg, Erlangen, Germany.

three-dimensional structures. Among these methods, different 3-D reconstruction approaches have become a useful tool in various applications in both the life and materials sciences. They result in three-dimensional displays which are particularly illustrative and instructive. Therefore, we now take a closer look at two of these 3-D reconstruction methods, one using an image series of specimen sections acquired in a light microscope, the second using electron tomography in a transmission electron microscope.

### 3-D Reconstruction using an image series of specimen sections

One commonly used method when dealing with 3-D reconstruction is to make a series of ultra-thin slices of the specimen being investigated. These slices are then dyed. The dye makes structures more easily recognisable and/or highlights specific parts. The slices are viewed one at a time beneath the microscope and drawn. These drawings are then enlarged to scale. In the past, a 3-D model was reconstructed layer by layer from pieces of cardboard cut according to the drawings. Alternatively, wax or plastic was used to

make the model. Today, this is greatly simplified by the computer assembling the virtual model. Special 3-D programmes calculate the three-dimensional model based on digitised image slices. This model is referred to as a 3-D reconstruction.

Today's powerful software offers 3-D processing, display and evaluation of two-dimensional image information. Ergonomic functions and flexible project management provide the user with the ability to reconstruct even the most complex models, and allow easy access to spatial views of the interiors of such structures. Up until now, these interior views were extremely difficult to generate. Box 16 shows the necessary steps of 3-D reconstruction, such as those used

for displaying embryonic growth processes in three dimensions. This approach is attractive for research conducted in other areas as well – such as the materials sciences.

### 3-D reconstruction by tilting the specimen

Tomography is another way of reconstructing the three dimensional (3-D) structure of a specimen from a series of two dimensional (2-D) micrographs. Some sample tomography applications include not only those for electron microscopy (called electron tomography) but also

\* eucentric is derived from the Latin for well-centered. It implies, e.g., in a goniometer and especially in a specimen stage, that the specimen can be tilted without moving the field of view. This capability is highly desirable for microscope stages.

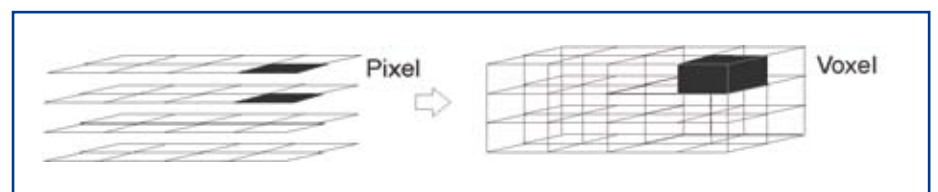


**Fig. 61:** This is how a two-dimensional pixel (picture element) is expanded to a three-dimensional voxel (volume element).

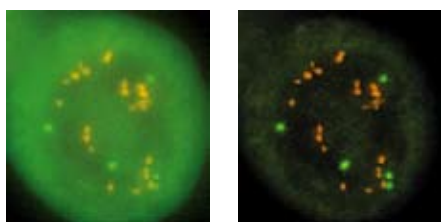
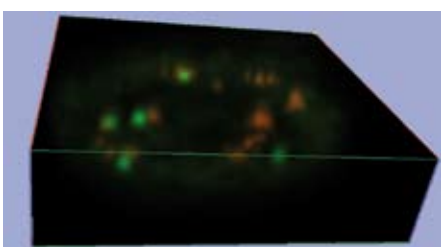
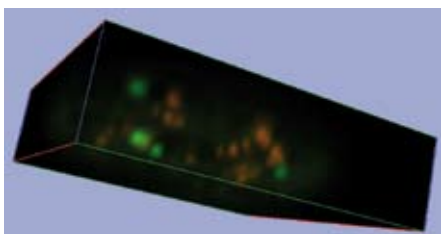


**Fig. 62:** Human breast cancer tissue labelled with a probe against the HER2-gene (Texas Red) and Chromosome 17 (FITC).

Upper left: Maximum intensity projection of 25 frames,  $\lambda(\text{FITC}) = 518 \text{ nm}$ , numerical aperture (NA) = 1, z spacing ( $\Delta z$ ) = 0.18.

Upper right: Blind deconvolution applied to both channels. Left: Maximum intensity projection.

When the volume-rendered structure is seen from two different angles, the spatial composition of the fluorescence signals is shown.

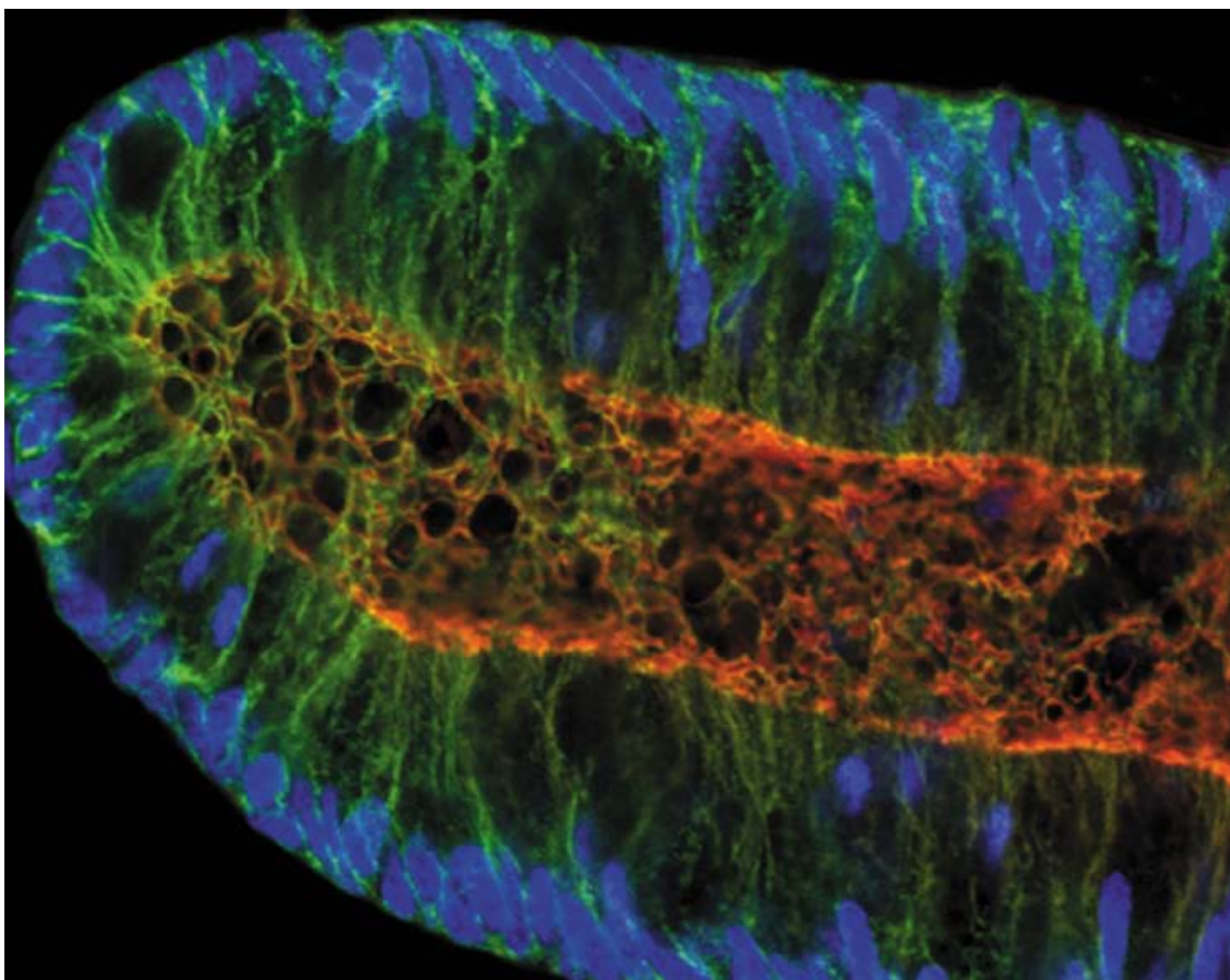


computerised axial tomography, (CAT) – familiar to many in medical applications as Computerised Tomography (CT).

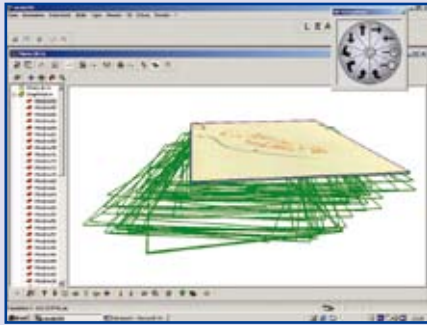
Computer tomography has long been a part of the standard repertoire for routine medical applications. Transmission electron tomography, however, has grown increasingly important as well in the last few years. Transmission electron tomography made possible what had seemed impossible in biology: 3-D imaging of interior cellular structures, just nanometres in size. This has become a reality due to a combination of new tech-

nologies – suitably equipped electron microscopes, high resolving and highly sensitive CCD cameras, increased computer processor performance and improved software.

The way in which electron tomography works is actually quite straightforward (see box 17). The specimen holder is tilted along an eucentric\* axis (if possible) and in the process, images are acquired from a wide range of angles. This guarantees that the 3-D structure will have adequate resolution along the three axes. Usually the specimen is tilted along a single axis from at least  $-60^\circ$  to  $+60^\circ$  with images (projections) recorded at equidistant increments of  $1^\circ$  or  $2^\circ$ . The images are acquired using a CCD camera and stored as a tilt stack. Due to effects such as sample shift, tilt of axis position or thermal expansion, the tilt stack has to be aligned before further processing can begin. Once the stack has been aligned, it is ready to be used for reconstruction. Reconstruction can be performed using different approaches. Two



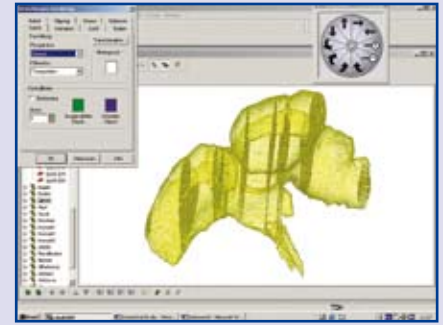
**Box 16: The steps involved in 3-D reconstruction using an image series of specimen sections**



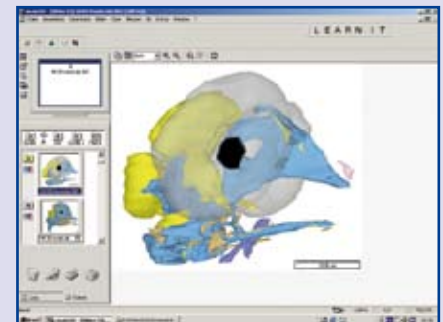
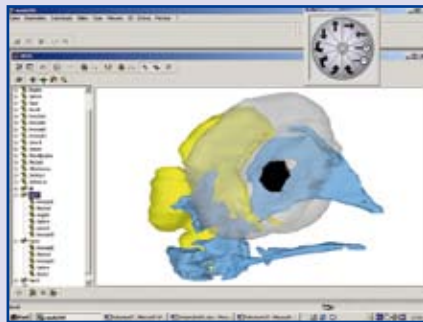
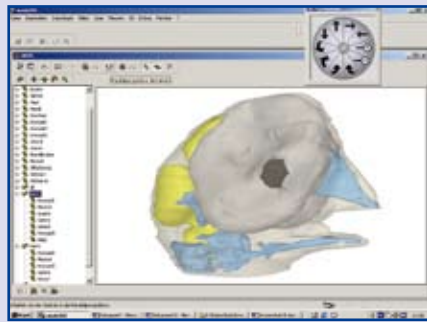
In the past, pieces of cardboard cut out by hand had to be glued together to make a 3-D model. Today this is all taken care of by the computer. First, the software digitally acquires microscope images of the series of image slices (or drawings are scanned into the computer, as in this case). The software then stacks these digitised slices. Any displacements or misalignments can be corrected interactively or semi-automatically.



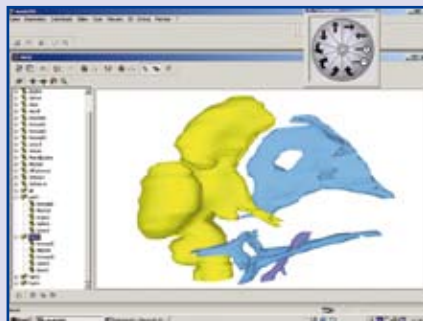
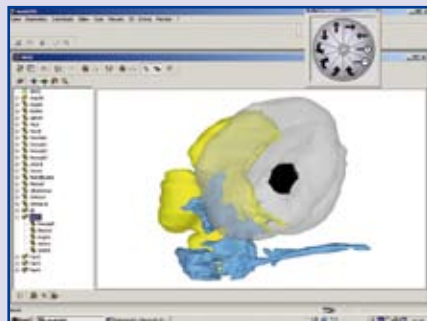
The contours of a tissue structure can be traced with the cursor or are automatically detected following a click of the 'magic wand' tool (a local threshold approach). The software then reconstructs the contours as polygons. This is a scanned drawing done at a stereo microscope. The procedure is exactly the same when using digital microscope images.



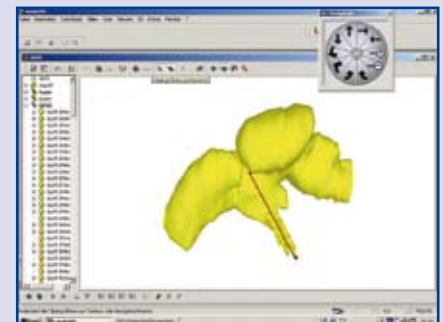
The software joins the two-dimensional polygons of the component layers to form spatial, three-dimensional structures. This is undertaken automatically. If necessary, manual corrections can be made. Using navigation tools, the object can be enlarged, reduced and rotated spatially in any direction.



This is a complete reconstruction of the skull of a quail embryo. To be able to investigate and measure precisely it is extremely important to be able to look inside the model. This is achieved by making individual parts transparent or fading them from view entirely.



Virtual specimen preparation: the digitally reconstructed skull of a quail embryo can be reduced to its component parts at any time. Virtual slices can also be generated in any direction.



Distance, polygonal length, area, volume and absolute position can all be measured directly within the 3-D view.

approaches available are called  $|w|$  filtering and (un-)weighted back projection via FFT. The resulting reconstructed image is stored and visualised as a z stack. Box 17 explains the steps necessary for the electron tomography process.

**The more dimensions – the more there is to see**

Many image-analysis methods, especially two- and three-dimensional approaches, have become well established and are

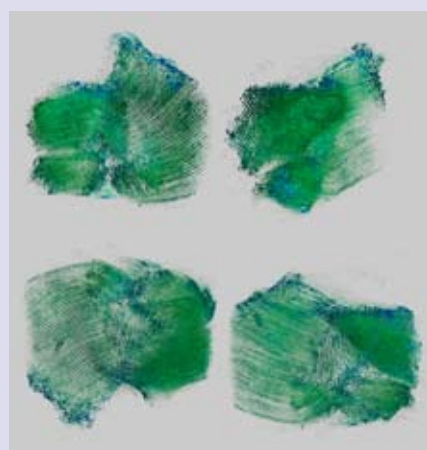
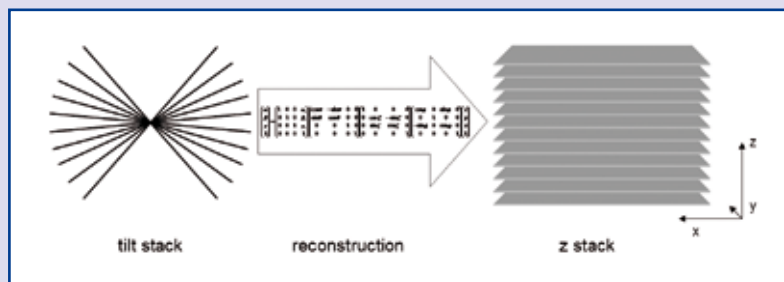
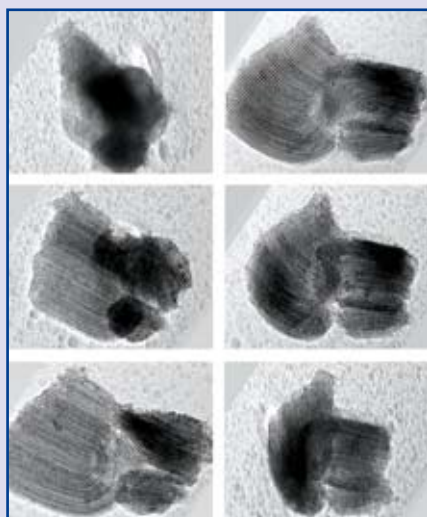
applied on a daily basis in both industrial and research applications. Innovative procedures involving even more dimensions with applications in the Life Sciences have also become available and are certain to become just as well established in the foreseeable future.

Wavelength is viewed as a fourth dimension in the field of fluorescence microscopy, as described above. Being able to differentiate wavelengths provides additional structural information. We have seen many new applications using this

technique. How the object being investigated changes over time is also of decisive importance in the Life Sciences. One particular reason for this is that this information may be crucial for assessing cell culture growth or for assessing how a fluorescent-labelled molecule behaves over time (see the paragraph „Fluorescence Lifetime Imaging Microscopy“ in the chapter „Shining Fluorescence Details“). In addition, there is further information which can be combined with x, y information efficiently. One example is



### Box 17: The steps involved in 3-D reconstruction via Electron Tomography (TEM).



Data collection for automated electron tomography involves a complex setup of TEM, CCD camera and a data gathering and processing system. Usually assembling the data would require a tilt of  $\pm 90^\circ$ . However, due to the geometry of the sample holder, or the thickness of the sample itself, the range of rotations is limited. This means that in practice, tilt angles ranging from  $-70^\circ$  to  $+70^\circ$  are recorded at equidistant increments. The image shows only 6 of at least 144 acquired images of the complete image stack. (Image courtesy by Oleg Abrosimov, University of Novosibirsk, Russia.)

A key feature offered by automated electron tomography is automatic alignment of the tilt series. Various algorithms can be used. The rigid axis is calculated using information such as magnification, tilt range and increment. The images are then stored in an aligned tilt stack.

Special reconstruction routines are used to generate a z-stack based on the data contained by the tilt stack.

Using visualising tools, 3-dimensional views inside the specimen becomes possible. The sequences can be animated and stored as files in .AVI format. The image shows 4 different views clipped from one .avi file.

energy loss. Energy loss plays a key role in fluorescence applications such as FRET (see the paragraph „Light as a Ruler“ in the chapter „Shining Fluorescence Details“). It is also used in several electron microscopy methods. Let's have a look at two of these methods: X-Ray Microanalysis and Energy-Filtering Transmission Electron Microscopy (EFTEM).

#### Combining morphological and chemical data

X-rays can be described as electromagnetic radiation with wavelengths ranging from  $10^{-9}$  to  $10^{-11}$  m or energy in the 10 eV – 100 keV range, respectively. X-rays are employed for element analysis in the field of biology, as well as in materials research. Characteristic X-rays and radiative deceleration of electrons within matter are recorded using special detectors. After correction for absorption, atomic weight and fluorescence, each sample section shows a characteristic spectrum. By scanning the sample and simultaneous recording of the X-ray signals, an element

distribution image can be recorded and visualised. Using image evaluation of these acquisitions, additional information becomes available which has previously been unattainable. This technique is in widespread use and referred to as EDX (Energy Dispersive X-ray Analysis) (fig. 63).

Combining digital image analysis with X-ray microanalysis makes it feasible to study and characterise the properties of new materials. This involves examining macroscopic material properties in relation to the microstructure. One application where this is essential is for improving and developing aluminium alloys, products and fabrication processes. To obtain an analysis that is statistically-reliable and representative requires a large number of samples. A TEM (Transmission Electron Microscope) with an integrated scanning mode can be used for analysing particles within the 10–300 nm range. This ensures that local resolution along with sufficient electron intensity is as required. The software controls and automates the entire acquisition and analysis process. This includes simulta-

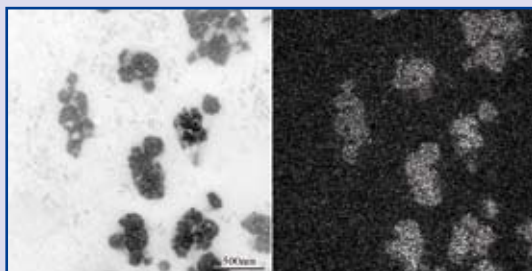
neous TEM and EDX analyser control, as well as analysis of the images acquired. The morphological data obtained within the context of the analysis is saved and displayed using tables and graphs. Subsequently, the automatic acquisition of the EDX spectra – at the centre of the particles being investigated – takes place. Data is also saved and quantified automatically. The proportion of the exudation volume can then be determined in conjunction with a layer-thickness measurement. These results can provide researchers with important micro-structural information (fig. 64).

#### Combining local data with energy loss data

The capacity for analysing multidimensional images is becoming more and more relevant. This includes image series of energy-filtering electron microscopy. EFTEM (energy-filtering TEM) image contrast occurs primarily due to the electron scattering within the sample – as is the case with the conventional TEM (box 18). Whereas conventional TEM

### Box 18: How is an elemental map of iron generated?

EFTEM stands for Energy-Filtering Transmission Electron Microscope. The electron beam of the EFTEM is transmitted through the sample (here, an ultra-thin section of brain tissue) and generates a magnified image of the sample in the imaging plane. The built-in energy filter makes it possible to generate electron-spectroscopic images (ESI). If the energy filter is set to 725 eV, for example, only those electrons reach the imaging plane that have an energy loss of 725 eV (while travelling through the sample). All other electrons are blocked by the energy filter.



725 eV is the characteristic energy loss of an electron from the beam when it 'shoots past' an iron atom at close proximity and causes a specific kind of inner-shell transition. The energy filter allows such electrons to pass through. These electrons contribute to image generation in the imaging plane. Unfortunately, other electrons manage to make it through as well. These also contribute to the image. These electrons have, however, coincidentally lost 725 eV – due to getting 'knocked about', i.e., multiple impacts occurring while the electrons pass through the sample. Without these coincidental electrons, the ESI image at 725 eV would be a straightforward elemental map of iron. This means that the image would show how iron is distributed throughout the sample.

The elemental map can be calculated using multiple ESI images. Using what is known as the 3-window method, 3 ESI images are acquired. The first one is at 725 eV, the second and third ones at somewhat lower energy losses. The second and third images are used to compute a 'background image'. This is then subtracted from the first image. This is how any background interference is removed from image number one (made up of all the contrast components caused by the coincidental electrons referred to above). The result is the desired elemental map of iron. This can now be used for making quantitative measurements.

Iron apparently plays a significant role in Parkinson's disease. Using an electron microscope, it can be shown how iron concentration has increased tremendously in the diseased part of the midbrain. The image on the left is an electron-spectroscopic image of an ultra-thin section taken from the substantia nigra\*\* of a Parkinson's patient (inverted display). The dark areas represent the neuromelanin. The image on the right is the elemental map of iron computed using the 3-window method. The light areas show where iron has accumulated. The quantitative evaluation in the example shown above indicates a concentration of iron that is three times as high as what it would be in the brain of a healthy person. (A LEO 912 AB EFTEM was used (acceleration voltage of 120 kV, electron energy loss of 725 eV) along with analySIS TEM EsiVision image-analytical software. (by Prof. N. Nagai and Dr. N. Nagaoka))

\*\*substantia nigra: is located in the midbrain and is a layer of large pigmented nerve cells. These cells produce dopamine and their destruction is associated with Parkinson's disease.

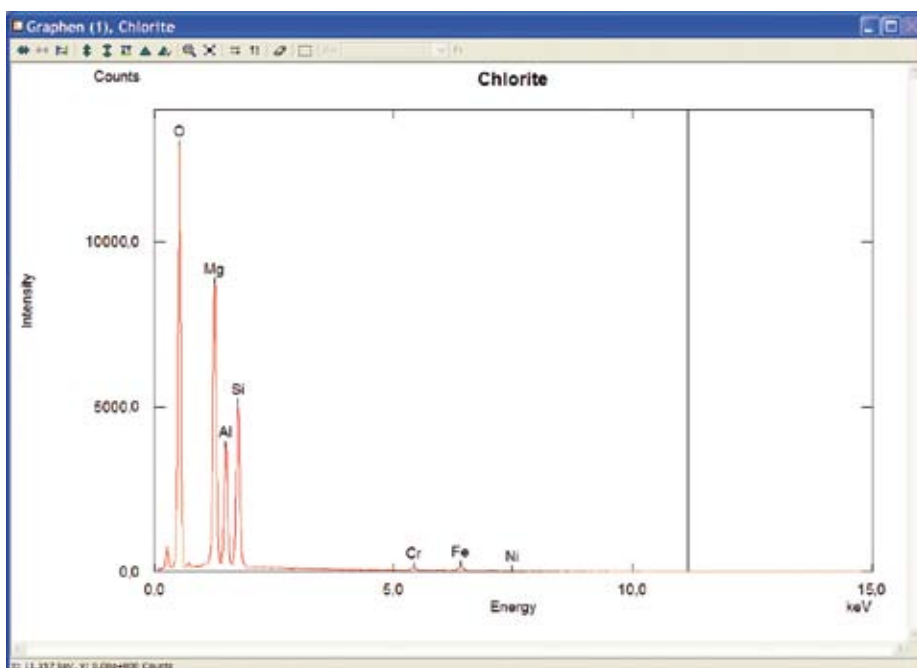


Fig. 63: Typical EDX spectrum.

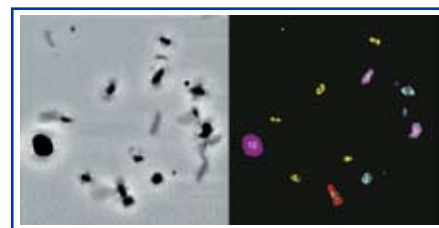


Fig. 64: a) Acquisition of an aluminium exudation, b) image following detection and classification. Chemical analysis is conducted following morphological evaluation.

contrast is caused by selecting the angles of the scattered electrons, the electrons within the EFTEM undergo an additional energy selection: using a spectrometer. Only electrons of a certain energy loss are selected (from the spectrum of the transmitted electrons) – the contrast-reducing portions are not visible. This means that only those electrons with a specific energy loss contribute to the acquisition. Thus the result offers enhanced contrast for all types of acquisition. Because this method does not affect local resolution, thin samples and those with no contrast, as well as frozen or unconventionally thick samples can be acquired with excellent contrast. Furthermore, this approach enables one to also select electrons with very specific scattering behaviour, thus yielding structural or element-specific contrast within the image. Images such as these provide new information on the sample that used to be inaccessible.

Control and remote control of the electron microscope for acquiring, displaying and analysing the images and spectrums is undertaken by special software. Much of the information can only be obtained via computer-supported processing and analysis. This method is used in the biomedical field, for example to demonstrate the presence of mineral particles in human lung tissue or when investigating diseases involving excessive accumulation of iron. This method has become greatly prevalent in the materials sciences as well: e.g., primary influences on the mechanical properties of steel – i.e., secondary phases, such as exudations or grain-boundary phases (carbide, nitride or also intermetallic phases). Determining the exact chemical composition, size, distribution and density is most important. This information can be obtained via the EFTEM method. Conventional methods are useless in this context.